

Long-path supercontinuum absorption spectroscopy for measurement of atmospheric constituents

David M. Brown, Kebin Shi, Zhiwen Liu, and C. Russell Philbrick

The Pennsylvania State University, Department of Electrical Engineering, University Park, PA 16802, USA

*Corresponding author crp3@psu.edu

Abstract: A supercontinuum source has been proposed as a new tool for measurement of minor species concentrations on long paths through the atmosphere. The present work describes results from recent experiments that demonstrate the potential for Differential Absorption Spectroscopy (DAS) and Spectral Pattern Recognition Differential Absorption Lidar (SPR-DIAL) measurements utilizing a supercontinuum source. As an initial example of this measurement approach, the results include the quantification of water vapor concentration through indoor and outdoor path absorption measurements using a collimated supercontinuum source. Experimental spectra are compared with equivalent simulations from MODTRAN™ versions 4 and 5 to examine the water vapor band between 1300 and 1500 nm to demonstrate the feasibility of the approach.

©2008 Optical Society of America

OCIS codes: (010.0280) Remote Sensing and Sensors; (010.3640) LIDAR; (010.1300) Atmospheric Propagation

References and links

1. R. A. Baumgartner and R. L. Byer, "Continuously tunable IR lidar with applications to remote measurements of SO₂ and CH₄ (E)," *Appl. Opt.* **17**, 3555-3561 (1978).
2. P. Weibring, C. Abrahamsson, M. Sjöholm, J. N. Smith, H. Edner, and S. Svanber, "Multi-Component Chemical Analysis of Gas Mixtures Using a Continuously-Tuneable Lidar System," *Appl. Phys. B* **79**, 525-530 (2004).
3. U. Platt, "Differential Optical Absorption Spectroscopy (DOAS)," in *Air Monitoring by Spectroscopic Techniques*, M. Sigrist, ed. (John Wiley & Sons, Inc. 1994).
4. H. Wille, M. Rodriguez, J. Kasparian, D. Mondelain, J. Yu, A. Mysyrowicz, R. Sauerbrey, J.P. Wolf, and L. Woste, "Teramobile: a Mobile Femtosecond-Terawatt Laser and Detection System," *Eur. Phys. J.: Appl. Phys.* **20**:3, 183-190 (2002).
5. G. Méjean, J. Kasparian, E. Salmon, J. Yu, J. P. Wolf, R. Bourayou, R. Sauerbrey, M. Rodriguez, L. Wöste, H. Lehmann, B. Stecklum, U. Laux, J. Eislöffel, A. Scholz, A. P. Hatzes, "Towards a Supercontinuum-based Infrared Lidar," *Eur. Phys. J. Appl. Phys. B* **77**, 357-359 (2003).
6. R. Bourayou, G. Méjean, J. Kasparian, M. Rodriguez, E. Salmon, J. Yu, H. Lehmann, B. Stecklum, U. Laux, J. Eislöffel, A. Scholz, A. P. Hatzes, R. Sauerbrey, L. Wöste, and J. Wolf, "White-light filaments for multiparameter analysis of cloud microphysics," *JOSA B* **22**, 369-377 (2005).
7. M. Cecilia Galvez, M. Fujita, N. Inoue, R. Moriki, Y. Izawa, and C. Yamanaka, "Three-Wavelength Backscatter Measurement of Clouds and Aerosols Using a White Light Lidar System," *Jpn. J. Appl. Phys.* **41**, L284-L286 (2002).
8. W. Wadsworth, N. Joly, J. Knight, T. Birks, F. Biancalana, and P. Russell, "Supercontinuum and four-wave mixing with Q-switched pulses in endlessly single-mode photonic crystal fibres" *Opt. Express* **12**, 299-309 (2004).
9. R. R. Alfano, *Supercontinuum Laser Source* (Springer Verlag, New York, 1989).
10. J. Begnoché, "Analytical Techniques for Laser Remote Sensing with a Supercontinuum White Light Laser" The Pennsylvania State University M.S. Thesis, 2005.
11. A. Berk, T. W. Cooley, G. P. Anderson, P. K. Acharya, L. S. Bernstein, L. Muratov, J. Lee, M. J. Fox, S. M. Adler-Golden, J. H. Chetwynd, M. L. Hoke, R. B. Lockwood, J. A. Gardner, and P. E. Lewis, "MODTRAN5: A reformulated atmospheric band model with auxiliary species and practical multiple scattering options," in *Algorithms and Technologies for Multispectral, Hyperspectral, and Ultraspectral Imagery X*, Proc. SPIE **425**, 341 – 347, 2004.

12. C. R. Philbrick, Z. Liu, H. Hallen, D. Brown, and A. Willitsford. "Lidar Techniques Applied To Remote Detection of Chemical Species in the Atmosphere," Proc. International Symposium on Spectral Sensing Research (ISSSR), 2006.
 13. D. M. Brown, A. Willitsford, K. Shi, Z. Liu, and C. R. Philbrick, "Advanced Optical Techniques for Measurements of Atmospheric Constituents," in *Proceedings of the 28th Annual Review of Atmospheric Transmission Models*, Lexington MA, June 2006.
 14. R. E. Warren, "Optimum detection of multiple vapor materials with frequency-agile lidar," *Appl. Opt.* **35**, 4180-4193 (1996).
 15. S. Yin and W. Wang, "Novel algorithm for simultaneously detecting multiple vapor materials with multiple-wavelength differential absorption lidar," *Chin. Opt. Lett.* **4**, 360-362 (2006).
 16. C. R. Philbrick, "Raman Lidar Characterization of the Meteorological, Electromagnetic, and Electro-optical Environment," *Proc. SPIE* **5887**, Lidar Remote Sensing for Environmental Monitoring VI, 85-99 (2005).
-

1. Introduction

Classically, multiple lasers with fixed wavelengths or tunable lasers are used in DIAL lidar systems to rapidly provide absorption measurements between on-line and off-line spectral features. Baumgarter, et al. for example, was successful in many measurements of atmospheric pollutants in the late 1970s [1]. The work, which was primarily focused on the remote detection of SO₂ and CH₄, was successful in detecting atmospheric background levels of CH₄ over a 5.4 km path length, and was typically able to observe SO₂ at levels near 100 ppm [1]. Since the 1970s, tunable laser technology has advanced dramatically. An example of this evolution is the study performed with midwave infrared tunable lasers by Weibring et al., published in 2004 [2]. Using a newly developed fast-switching, frequency-agile optical parametric oscillator (OPO) lidar transmitter, Weibring et al. were capable of measuring increased concentrations of methane, ethane, propane, and butane from a distance of 50 m. This example demonstrated the concept of a multi-wavelength lidar system with multivariate analyzing techniques for hydrocarbon gas mixtures. The system was successful in measuring the individual concentrations of several species; however, measurements in gas mixtures with overlapping spectral features were more complicated due to a limited number of uncontaminated wavelength comparisons [2].

An alternate technology, published by Platt et al. and other groups, focuses on differential absorption instruments utilizing incoherent sources. These instruments have similar capabilities to tunable laser systems; however they have far more wavelengths available for differential comparisons [3]. The incoherent sources are normally high intensity lamps (Xenon arc), which perform quite well over a variety of measurement paths, and have some advantage in populated areas where laser use is more restrictive. Some of the most compelling atmospheric measurements with this technology are those measurements reported by Platt et al., which used a geometry that placed the transmitter and receiver at opposite ends of a kilometer long path [3]. The study demonstrated that differential absorption measurements are feasible over ranges of hundreds of meters in length using this approach. The difficulty in the collimation of lamp sources limits the accuracy as ranges are increased from hundreds of meters to many kilometers.

A method that reduces the limitations of lamp source remote sensing instruments and still preserves the advantages of broadband operating systems is a terawatt femtosecond lidar system developed in a joint research venture between French, Swiss and German universities [4,5]. This sensor, referred to as "Teramobile," uses ultra short high energy laser pulses to probe the atmosphere for various species and for aerosol studies [6]. By generating a supercontinuum, or white light spectrum at a predetermined range, the system is able to observe the differential absorption of many atmospheric species between the ground and several kilometers in altitude. The mechanism that creates the supercontinuum, however, requires very large localized electric fields within the path of the transmitted laser. The fields give way to a host of nonlinear effects that broadens the pulse in the wavelength regime, thereby creating the white light spectrum. Controlling the light (in terms of stability of the wavelength regime), however, can be difficult due to the varying atmospheric non-linear effects introduced in the region of the focused femtosecond pulses. Additionally, as the name

suggests, the transmitted peak power per pulse is on the order of terawatts and could impose some limits on urban measurement applications. Other approaches have been able to generate a supercontinuum (via femtosecond lasers) within a cell to perform atmospheric characterizations of aerosols [7]. Using localized cells to generate a supercontinuum introduces more control into the generation process. These advantages in control are important for making time sequence measurements of atmospheric phenomena, and are similar to those shown when generating supercontinuum spectra in photonic crystal fibers [8].

Supercontinuum Absorption Spectroscopy (SAS) presents an alternate solution that can provide some advantage in terms of fabrication, operation, power requirements, and cost effectiveness. By using photonic crystal fibers and nanosecond pulses, we are able to generate a supercontinuum spectrum within the transmitter, and therefore remove the requirements of self focusing in the atmosphere used in the Teramobile system. This technique can be used at ranges of 10 m to 10 km with minimal system modification, while transmitting nearly 9 orders of magnitude less peak power. Further changes in the geometry have simplified the optical alignment by arranging the transmitter and receiver in a monostatic manner. Adopting a variant of the design presented by Platt et.al [3], we place the transmitter and receiver of the SAS system at the same location in a collinear configuration. Using this geometry, we transmit the supercontinuum beam from our roof laboratory to adjacent buildings where retroreflector targets are positioned. The retroreflector targets direct the beam back to the receiving telescope which transfers the light to a spectrometer for analysis. This approach allows for the collection of a large percentage of the transmitted signal and when combined with a sensitive spectrograph, it can generate absorption spectra with sufficient signal to background using sub-second integration times.

With these advantages, the SAS system is capable of answering the research needs for highly accurate spectroscopic measurements in areas where laser visibility and/or eye-safety issues could impose restrictions. Details of the design and sample datasets are discussed in this paper. Additionally, we have explored data analysis algorithms for multiple wavelength DIAL lidar systems and applied a variant of one algorithm to indoor and outdoor SAS spectra of water vapor to demonstrate the measurement approach.

2. Supercontinuum source

The SAS transmitter in our system utilizes a low power, relatively low cost supercontinuum source. By coupling sub-nanosecond laser pulses from a passively Q-switched microchip laser (JDSU NP-10620-100, wavelength at 1064 nm, average power ~ 70 mW) into a 18 m photonic crystal fiber (Blaze Photonics SC-5.0-1040) we are able to generate supercontinuum white light [8, 9]. When using 40X microscope objectives to focus the light into the PCF and also to re-collimate, the typical supercontinuum output average power is 16 to 18 mW. The pump laser has a repetition rate of 8 kHz with a peak power per pulse of about 8.75 μ J per pulse which lends to four-wave mixing as the primary mechanism responsible for the creation of broadband laser light. A typical spectrum of the supercontinuum source used for the absorption investigations described in this work begins near 500 nm and extends into the near infrared beyond 1600 nm as shown by Fig. 1(a). During the spectral measurement of the full range of the supercontinuum source, the spectrum was collected by collimating the supercontinuum output and focusing the light down via a 20X microscope objective into a multimode fiber. This fiber was then connected to an Ando (now Yokogawa) optical spectrum analyzer (AQ6315E) input, and the wavelength region was scanned in approximately five seconds. Fig. 1(b) shows the raw supercontinuum output from the photonic crystal fiber, while Fig. 1(c) shows the rainbow formed from the collimated supercontinuum passing through a 1100 lines/mm grating.

3. Laboratory path measurement

Our first experiments utilized the supercontinuum source to measure atmospheric water vapor content along a folded path in the laboratory environment [10]. This result was then compared to the MODTRAN™ [11] simulation result for the water vapor absorption band in the 1.3 to 1.5 μm region.

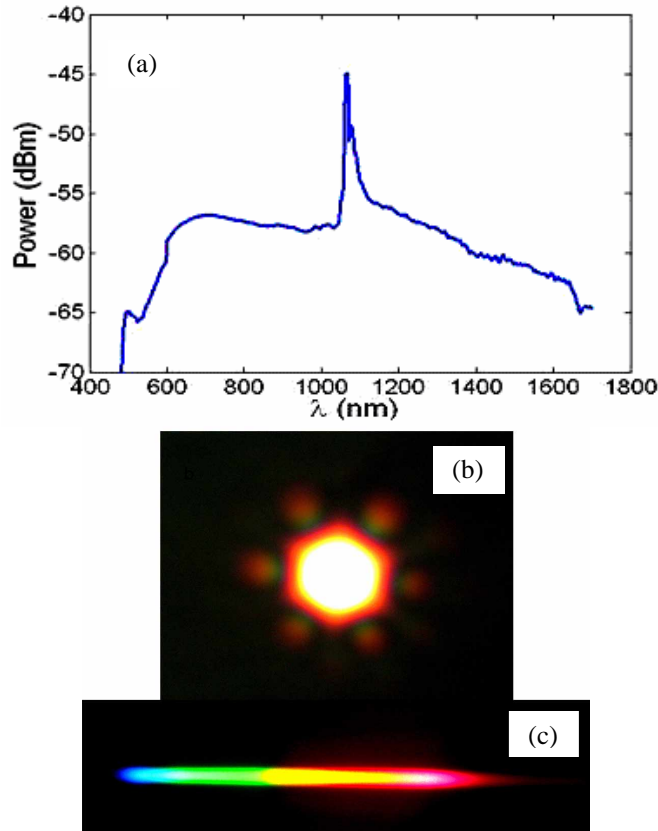


Fig. 1. (a) Supercontinuum source spectrum; (b) The far field pattern of the supercontinuum spectrum generated from a photonic crystal fiber; and (c) Rainbow observed after collimated light passes through a prism.

3.1 Experimental setup and selection of wavelength region

The indoor laboratory supercontinuum absorption measurement traversed a 20 m path before being coupled into the Ando spectrometer for data collection. Due to the beam traversing a relatively short path length through filtered laboratory air, the experiment minimized aerosol scattering, which is very prominent in the outdoor measurement cases. A simple experimental setup, shown in Fig. 2, was employed to allow the collimated beam to traverse the absorption path and then be coupled into the Ando optical spectrometer via a 20X microscope objective, and a 3 m multimode fiber optic connection. Typically, sub second scan times on the spectrometer were sufficient to capture the wavelength range of interest in low resolution for indoor measurement cases of water vapor absorption spectra. When operated in this mode, the Ando spectrometer has a data collection range of roughly 200 nm; therefore, a spectral region of interest is specified prior to carrying out an experiment. To set the wavelength range for the Ando spectrum analyzer, we examined the horizontal transmission for a 20 m path using an atmospheric transmission model. The MODTRAN™ model is convenient for

determining the approximate transmission profiles for cases typical of atmospheric conditions (temperature, pressure, constituent concentration, aerosol distributions, path length, etc.). Based on our examination of the MODTRANTM model, we configured the Ando spectrometer to examine the water vapor absorption band in the near infrared between 1300 and 1500 nm (~ 7700 and 6700 cm^{-1}) because of the spectral features and absorption magnitude expected there.

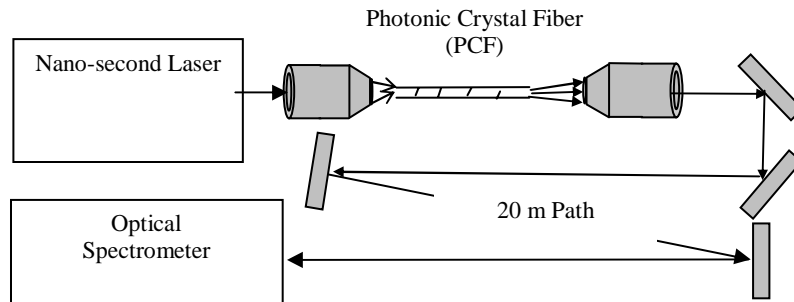


Fig. 2. Experimental setup used to measure water vapor spectrum with a supercontinuum source.

3.2 Experimental result compared to MODTRANTM simulation

The results from the normalized experiment data are compared with the model output of the MODTRANTM 4 in Fig. 3. The experimental data was captured with a resolution of 0.2 nm set in the Ando spectrometer, with a sampling increment of 0.05 nm. In the vicinity of 1.4 μm , these settings correspond to an equivalent MODTRANTM 4 resolution of 1 cm^{-1} with a sampling increment of 0.25 cm^{-1} . To acquire experimental absorption path measurements, a reference spectrum was used to normalize the experimental data sets through a polynomial fit of the instrument function. Following the normalization, the implemented routine ensures that the slit widths are equivalent between the experiment and the model. The routine first calculates absorption spectra from HITRAN cross sections with a range of slit widths in the vicinity of the approximate match. The process then takes the inverse of these calculated absorption spectra, and tracks the correlation with the experimental data set. The slit width that corresponds to the maximum correlation is then selected as the optimal solution for the experimental case. The selected slit width is then used to create the appropriate MODTRANTM simulation result. Alternatively, if we intend to examine the spectra in a coarser resolution than when it was originally collected, we simply smooth the data with the appropriate slit width and calculate the appropriate cross sections. The baseline noise present in the measurement shown by Fig. 3. is likely due to the propagation of higher order modes throughout the fiber optics present in the optical path in addition to instrumental noise. In later experiments, this effect was reduced by tightly coiling any fiber optics used in the system so higher order modes would leak from the core-cladding interface (mode filtering.)

After comparing with MODTRANTM 4 as shown in the example in Fig. 3, we then compared higher resolution measurements with the beta version of the MODTRANTM 5, which has a resolution capability of 0.1 cm^{-1} . In these cases, the resolution of the spectrometer was configured to be 0.08 nm, with a sampling increment of 0.02 nm. In the vicinity of 1.4 μm , these settings correspond to an equivalent MODTRANTM 5 resolution of 0.4 cm^{-1} with a sampling increment of 0.1 cm^{-1} . Figures 4 and 5 show examples of these measurements along with the model comparisons when the resolution of the MODTRANTM 5 simulation was adjusted to the settings of the Ando spectrum analyzer. Results from the analysis of the spectral correlation between the experimental data set and MODTRANTM simulation outputs generally agree as shown by Figures 4 and 5. Additionally, the result from the 0.1 cm^{-1} simulation is included in Fig. 5 to show the full capability of the MODTRANTM 5

model. This provides additional comparison to examine the spectral changes associated with the instrument resolution and slit width.

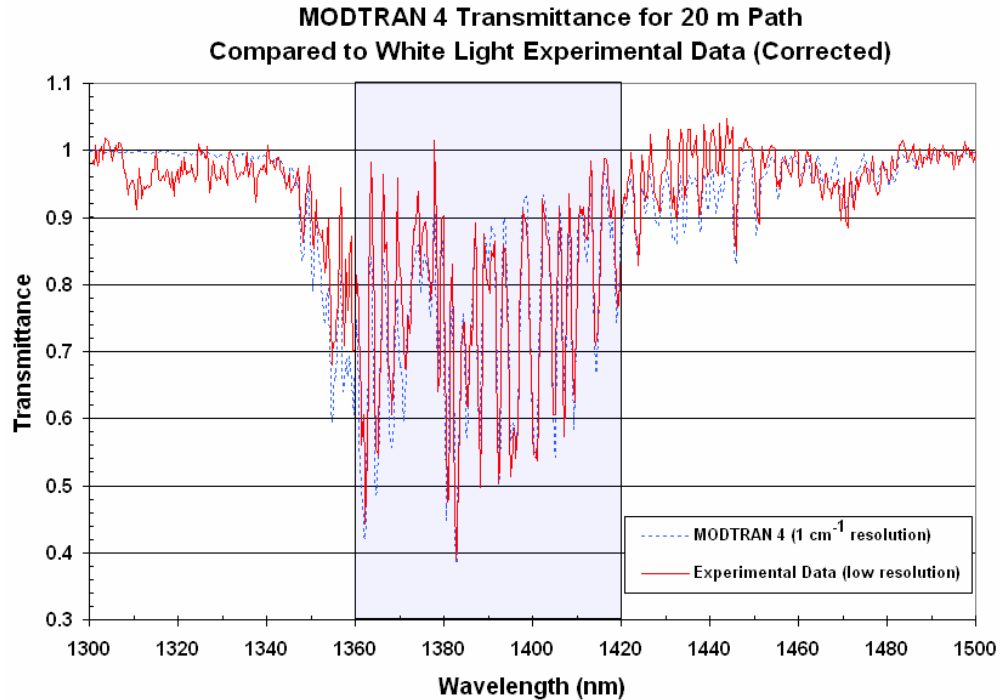


Fig. 3. Normalized water vapor transmittance 1300-1500 nm measurements using the supercontinuum laser (red) are compared when the spectrometer slit is set for the 1 cm^{-1} resolution corresponding with of MODTRANTM 4 (blue).

A quantitative examination of the experimental results presented above is found in section 4.2 of this work where collected datasets are used to calculate a relative humidity concentration of air in the laboratory. We validate the experimental result using relative humidity measured by a sling psychrometer and a digital humidity meter present in the laboratory. For the example presented, the percent difference in relative humidity was 2%.

To create the MODTRANTM result shown in figures throughout this section, we needed the water vapor concentration present in the laboratory at the time of experimentation, which could be acquired through the developed data processing approach, or through the ground truth, point measurements. The figures shown above reflect simulations that were created using the ground truth measurements, which can account for some of the differences. Pressure and temperature effects on the spectral agreement and data processing approach were not explored in this study as the MODTRANTM simulations and calculated absorption spectra used for the data analysis utilized ground truth temperature and pressure datasets acquired at the time of experimentation. Finer resolution experimentation would increase the influences of pressure and temperature effects on the magnitude and shape of the absorption features under investigation.

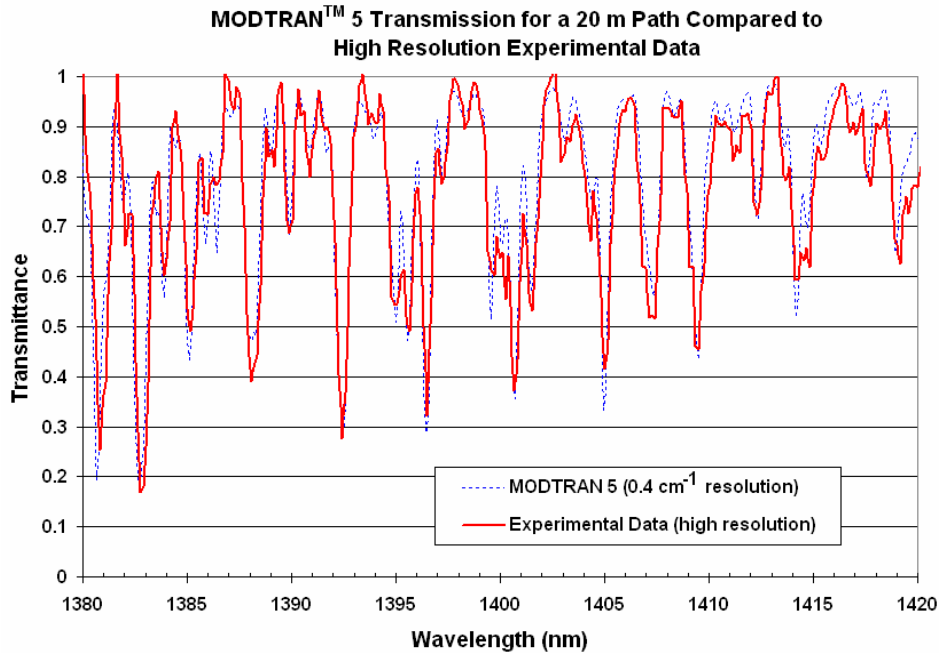


Fig. 4. Water vapor transmittance 1380-1420 nm experimental measurements (red) compared with MODTRAN™ 5 simulation (blue), with resolution matched to the instrument 0.4 cm⁻¹ parameter.

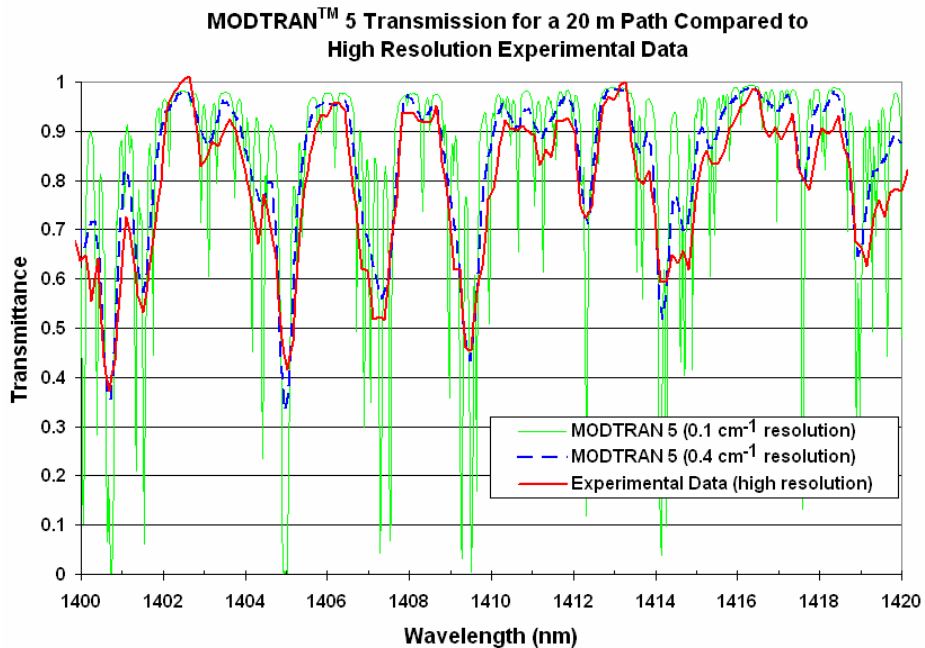


Fig. 5. Water vapor transmittance 1400-1420 nm experimental measurement (red) compared to MODTRAN™ 5 simulation with parameters selected to match the sensor (blue). The highest resolution available (0.1 cm⁻¹) for MODTRAN™ 5 simulations (green) is also shown for reference.

4. Data analysis algorithms

While MODTRANTM provides us with the toolset required to quickly simulate a set of reference spectra for various concentrations of water vapor and other species, a more robust approach for calculating gas concentrations from measurements is required. In particular, a real-time instrument requires a rapid processing scheme to determine a total concentration path length (CPL). An appropriate CPL algorithm should optimize the correlation coefficient between an experimentally measured and simulated spectrum using many features in the spectral region, rather than just two wavelengths traditionally used in DIAL analysis. Additionally, when the spectrum contains several absorbing species with unknown concentrations, the analysis algorithm must be sufficiently robust that the responses of interferences are also determined during the calculation of the target CPL. Moreover, in real world applications, the “interferents” are often additional targets of interest. For these reasons, we have implemented a data processing algorithm that provides the framework for detection and quantification of several mixed vapors in a composite response. Unlike typical frequency agile lidar systems, where the composite response would consist of a number of carefully chosen laser lines to be used in a DIAL analysis, implementation of a supercontinuum source provides a capability to measure several species simultaneously, using the mixture of on-line and off-line features in the analysis. This approach provides the ability to perform simultaneous detection of multiple vapors with strong spectral overlap, i.e. Spectral Pattern Recognition DIAL (SPR-DIAL) [12,13].

Similar to DOAS approaches, the following algorithmic approach has the capability to estimate the atmospheric concentration of multiple spectrally overlapping features. Even though our current datasets do not possess absorption structure from multiple overlapping species, we have chosen to analyze the data using such an approach due to the inherently stable nature of maximum likelihood techniques, and to explore the functionality of such an algorithm with many wavelengths. Step one of the approach is to calculate the absorption spectra of each possible target species in spectral range. This is currently performed by utilizing HITRAN cross sections and atmospheric pressure and temperature measurements taken at the time of experimentation. While atmospheric temperature and pressure can be measured remotely through Raman [16] and DIAL lidar approaches respectively, the present work has focused on initial laboratory and outdoor measurements of water vapor concentration using local meteorological data for these parameters. The absorption spectra and experimental data spectral resolution are then matched before the algorithm is executed. The algorithm calculates the concentration of each possible target for a host of wavelength combinations. For a more detailed explanation of the core algorithmic approach, we refer the reader to the work of Warren [14] or Yin [15], as our approach is built on the fundamentals developed in these works. Ultimately the final concentration for each target is derived from the average of multiple algorithmic results from this core process. We must note, however, that if a species absorption spectra is not well known and its structure overlaps the spectral range under investigation, errors in concentration measurement of known species may occur.

4.1 SAS multi-wavelength algorithm

The multiple wavelength DIAL data processing algorithms combine the traditional DIAL remote sensing techniques and maximum likelihood statistical analysis techniques. Our analysis is built on the theoretical work of Warren [14], and is implemented following the procedure shown by Yin and Wang [15]. The algorithm does not require varied concentrations of the target species to be spectrally simulated in order to obtain a least squared fit, which can prove to be quite time costly and difficult to implement for multiple spectrally coinciding targets. Instead, starting with an initial guess of 0 ppm for the target or targets, the algorithm will iterate to an estimated CPL.

The work of Warren generalizes a two-wavelength single target methodology and evolves it to include multiple wavelengths and multiple targets [14]. However, the approach is still tied to the paradigm of computing the ratio of wavelength return pairs. Additionally, the

technique depends upon having the spectral data in a convenient form such as that available in MODTRANTM [11]. In subsequent sections, Warren derives an alternate method of detection and quantification based on likelihood ratio test methodology which directly utilizes the return signal of each wavelength. Although the approach is functional for multiple laser lines that are sufficiently separated in wavelength, the maximum likelihood estimation method (MLE) developed by Warren has been demonstrated by Yin and Wang to be very sensitive to initial offsets in the differential atmospheric transmission. The iterative algorithm for the calculation of target species CPL is performed for each wavelength pair in Warrens work, and thus produces estimation for CPL that is very sensitive to noise details [15]. The sensitivity to noise details (and eventually for the CPL calculation) is particularly enhanced for vapors whose spectra are highly structured, and this is typical of many targets of interest. The changes made by Yin and Wang to the MLE algorithm forego the iterative procedures for each wavelength pair. Starting with an initial CPL guess, they simultaneously solve for the noise covariance matrix, $\hat{\Lambda}$, and CPL of multiple vapors [15]. Following this procedure, the SAS algorithmic approach uses a complete array of wavelength specific target vapor absorption parameters, α , simulated signal, \hat{H} , and average SAS integrated measurements, $\bar{Q}(j)$, to solve for the main parenthesized component in Eq. 1. This modification is equivalent to looking at wavelength pairs concurrently, as a weighted sum of the entire set instead of as a set of individual estimations.

Subsequent to sampling the input data (both absorption spectra and composite experimental measurement) at the appropriate wavelengths, the algorithm performs an iterative procedure. After a number of iterations, the result approaches an estimated CPL for each target, l , if the target is present in the collected dataset. Equation 1 shows the MLE algorithm we use as the core processing step used to analyze the SAS data.

$$CPL_l = \frac{1}{n-1} \sum_{M=n-x}^n \left[\frac{\sum_{j=1}^M \left[\alpha_{jl} \hat{\Lambda}_1^{-1}(j, j) \left[\hat{H}_1 - \bar{Q}(j) - \sum_{l=1, l \neq l}^L \alpha_{jl} CPL_l \right] \right]}{\sum_{j=1}^M \left[\alpha_{jl} \hat{\Lambda}_1^{-1}(j, j) \alpha_{jl} \right]} \right] [ppm \cdot m] \quad (1)$$

We have, however, tailored the logic for calculating CPL to increase its robustness in analyzing real world data collects. Since we have many wavelengths containing information of the species, we enhance the accuracy of the calculated CPL by using a linearly spaced wavelength sampling scheme and following the convergence of the concentration calculation to a stable value. By picking a wavelength range of interest, and incrementing the number of laser wavelengths, M , from $n-x$ to n , our CPL result is quite robust as it is an average of the results for these cases.

4.2 Outputs of the SAS multi-wavelength algorithm

We have processed the data from the initial 20 m path experiments described in Sect. 3 using a composite absorption spectrum of water vapor and the MLE algorithm. In this case, the MLE converges to the concentration of water vapor present in the path. This concluded concentration, however, is a path averaged measurement, and thus does not necessarily reflect localized variations along the path. Figure 6 shows a schematic representation of the initial testing of the MLE algorithm. The figure shows a case where 50 linearly spaced wavelengths (red vertical lines) are used to sample the absorption spectra and collected experimental dataset between 1380 and 1420 nm. The result of the MLE algorithmic iteration is also shown in Figure 6. For this specific example, the procedure approximates the water vapor concentration to be approximately 10000 ppm for the 20 m path averaged measurement. Knowing that at the time of experimentation the relative humidity of the air in the laboratory environment was measured to be 37% at a temperature of 296 K, the equivalent concentration in ppm can be calculated through equation 2. The result is a concentration of water vapor of

10300 ppm. This agrees well with the initial result of the MLE algorithm, however, the conclusion is biased as the analysis has only been run with a single set of wavelengths. Stability in the CPL conclusion when multiple wavelength sets are used for MLE analysis provides a far more confident result.

$$C_{H_2O}[\text{ppm}] = 10^4 (RH) \frac{\text{Saturation Water Vapor Pressure}}{\text{Partial Pressure of Water}} = \frac{P_{H_2O}^o}{P_{H_2O}} \quad (2)$$

$$= 10^4 (RH) \exp \left[13.3185 \left(1 - \frac{373.15}{T} \right) - 1.976 \left(1 - \frac{373.15}{T} \right)^2 - 0.6445 \left(1 - \frac{373.15}{T} \right)^3 - 0.1299 \left(1 - \frac{373.15}{T} \right)^4 \right]$$

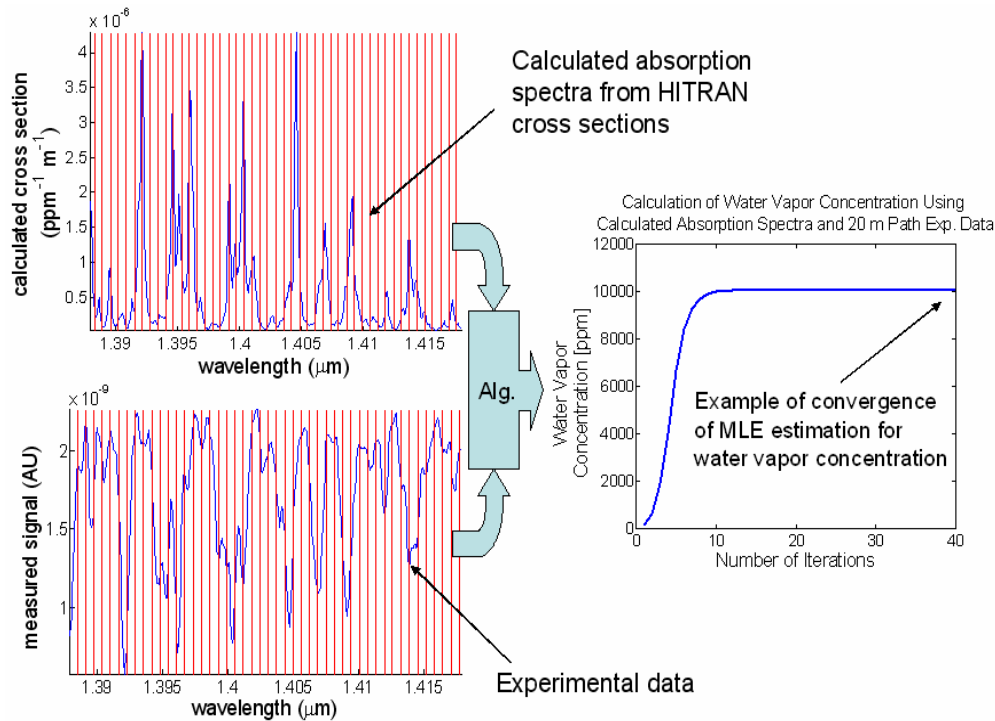


Fig. 6. Shown on the left is the calculated water vapor absorption spectrum (top) and experimental data (bottom). The red vertical lines are utilize a linearly spaced wavelength sampling scheme to feed spectral absorption information into the MLE algorithm. The algorithm iterates until it converges upon a best fit CPL (right), given the set of experimental data and absorption spectra of water vapor in a predetermined wavelength region.

Therefore, subsequent analyses use an array of cases employing linearly spaced selected wavelengths within the measurement region and start with a guess of 10000 ppm. A case study using up to 500 wavelengths is shown in Fig. 7. Beyond 200 linearly spaced wavelengths (initial zero concentration), the variation in the CPL result decreases and roughly varies between 2 and 5%. This yields an average resultant concentration of water vapor of 10900 ppm, which is about 2% different from the value of relative humidity determined from the point measurements within the laboratory. This difference is larger than desired, however, it is important to note that a one degree temperature change over the length of the path can result in a difference of this magnitude. Additionally, we note that the measurement volume is very different. The optical absorption measurement over a 20 m path compared with a laboratory point measurement of relative humidity should result in some difference.

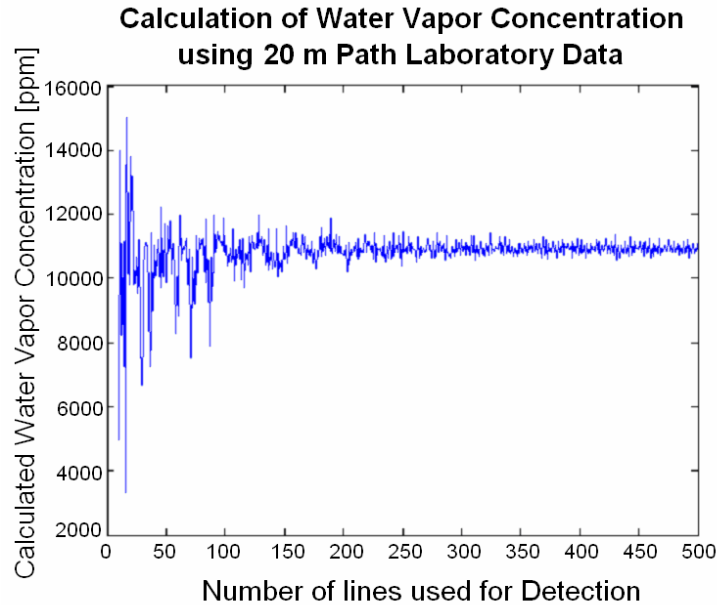


Fig. 7. Calculation of water vapor concentration showing the convergence using 10 to 500 laser lines for comparison.

5. Atmospheric path measurements

By ruggedizing our nanosecond VIS-NIR supercontinuum source and integrating it into a transceiver, the system evolved to a stand alone unit capable of making path absorption measurements outside of the laboratory and over ranges of hundreds of meters. We have demonstrated in the following that the 16 to 18 mW average transmitted power of the supercontinuum source system is sufficient enough to make highly accurate measurements of water vapor concentration along 300 m paths between building rooftops. Figure 8(a) shows the setup of the supercontinuum transceiver inside the door of our rooftop laboratory. The system utilizes a 114 mm diameter Newtonian telescope with a focal length of 450 mm. The fiber used to collect the reference and signal spectrums was standard multimode telecom fiber with a 0.22 numerical aperture. The scanning rate and integration setting of the spectrometer varied throughout outdoor experimentation due to variations in the supercontinuum output power, and atmospheric conditions. Typically, the time required to capture one scan of the spectral region of interest was on the order of 1 to 5 seconds. A subset of this collected dataset was then later used for analysis of water vapor concentration along the path. Figures 8(b) and 8(c) are images taken during the operation of the instrument. Figure 8(b) shows the scattered component of the supercontinuum return from a retroreflector observed from 150 m away, and Fig. 8(c) shows the PCF under optimal coupling and hence peak output power conditions. The highly nonlinear PCF spreads the 1064 nm pump wavelength over a range of wavelengths in the visible and near infrared parts of the spectrum by nonlinear optical processes.

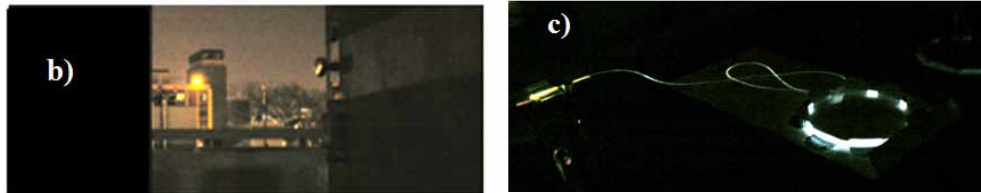
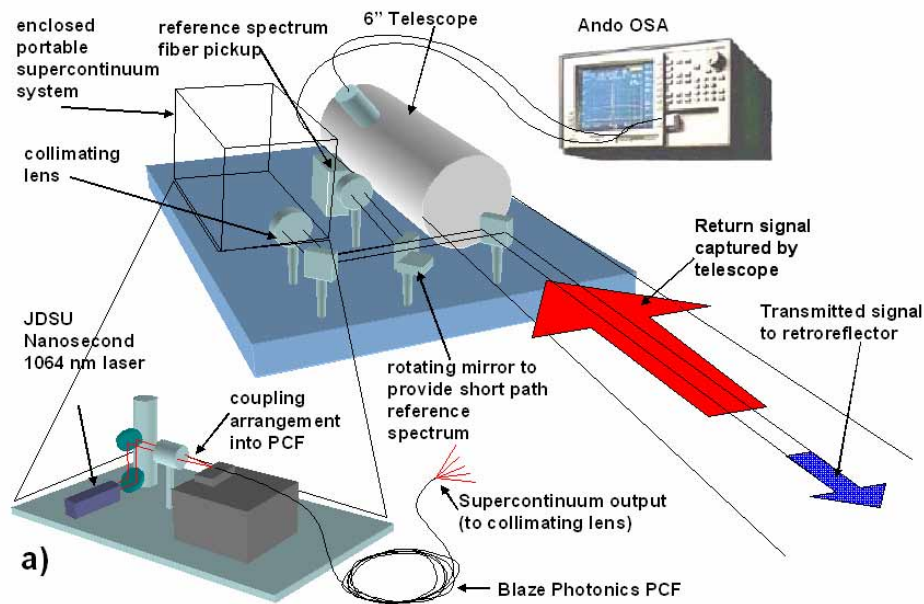


Fig. 8. (a) Experimental setup for long path SAS measurements; (b) view through the laboratory door shows the reflection of UV-NIR supercontinuum source from a 6" retroreflector located ~150 m away; (c) the wavelength spread of the supercontinuum light can be observed in the PCF, when it is properly tuned for maximum output power, it is spread in wavelengths through visible and near IR due to self phase modulation.

The spectral mapping of water vapor concentration along the path for a range of atmospheric conditions was obtained. The outdoor path measurements of water vapor generally agreed with the local meteorological measurements of relative humidity conducted within 0.5 km of the test site. The water vapor absorption features in the vicinity of $1.4 \mu\text{m}$ are clearly observed in comparison between the experimental data and a MODTRANTM simulation shown in Fig. 9. The water vapor absorption is so strong in the original wavelength range that no signal was detectable at the centers of several absorption lines in the transmitted supercontinuum beam between 1.380 and $1.420 \mu\text{m}$. To reduce the effects of this complete absorption on our concentration measurements, we performed our studies on absorption features selected from a range of lower absorption in the region from 1.434 to $1.439 \mu\text{m}$. We examined the same spectral region for two different measurement cases separated by a ten hour period. The MLE results are shown in Fig. 10. By taking the average concentration and standard deviation for MLE results utilizing 100 to 120 wavelengths, we conclude that the first data set provides a concentration of water vapor of 9582 ± 20 ppm, while the second data set provides 10793 ± 32 ppm. Figure 11 then compares this result to water vapor concentration recorded by the meteorological station nearby. The percent difference for these cases is at a maximum of 4 %.

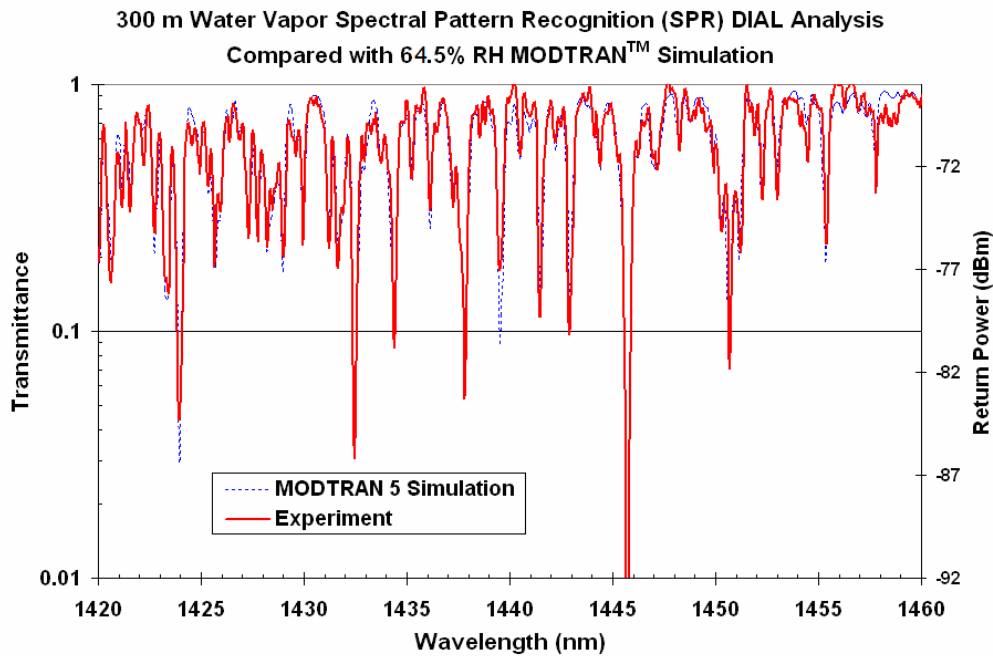


Fig. 9. Spectral measurement in the 1420 to 1460 nm infrared region with strong water vapor absorption features.

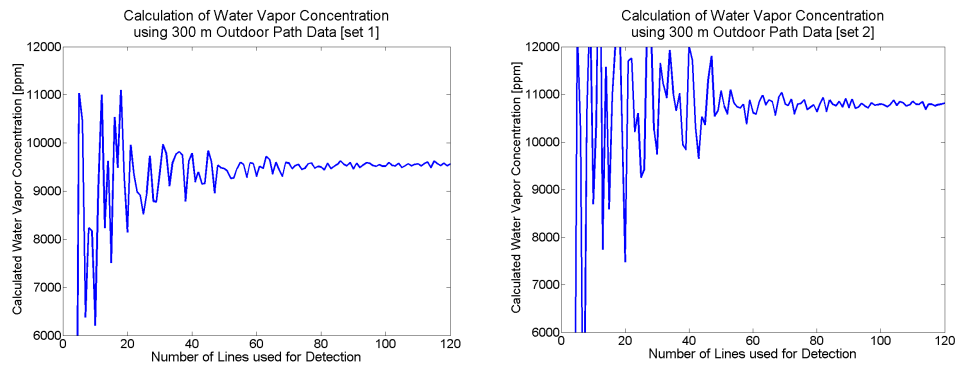


Fig. 10. Result of MLE algorithm for two 300 m path averaged measurements of water vapor.

6. Conclusions and outlook

By using the spatially coherent supercontinuum source, spectral mapping differential absorption techniques can be exploited for remote sensing purposes. A broadband supercontinuum source was demonstrated to remotely measure water vapor concentrations based upon the absorption features at NIR wavelengths for indoor and outdoor measurement cases. Remote measurements were then compared to nearby ground truth measurements and generally agreed within 3 to 5%.

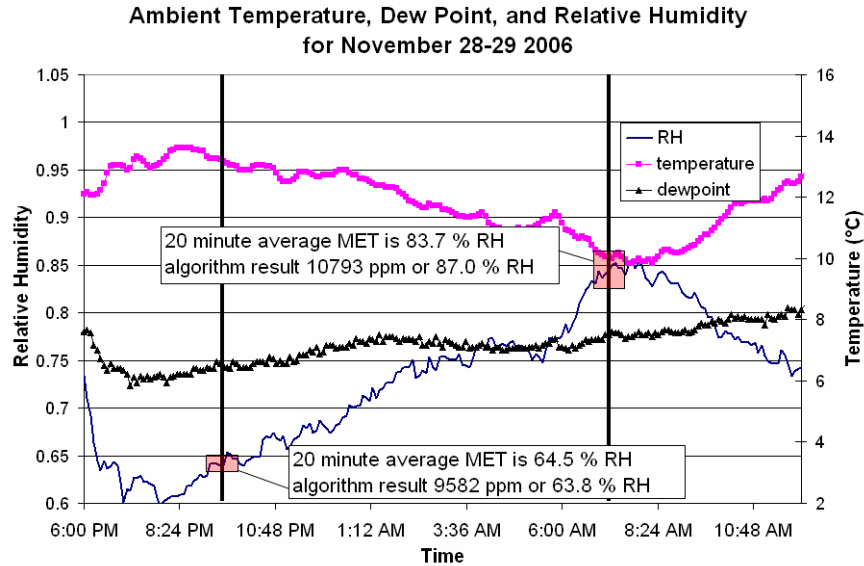


Fig. 11. Comparison of averaged MLE results to local MET data.

By rearranging the system measurement geometry and employing a long path absorption technique, we have developed a system that minimizes transmitted power and is still capable of urban pollution monitoring and/or emergency response mapping of chemical species. Although supercontinuum sources are not included specifically in the ANSI safety rating for this region, the low transmitted power required for supercontinuum absorption measurements is an advantage for many applications. Additionally, we suggest that highly accurate trace species measurements can be achieved with long path geometry between ground and space. By employing longer integration times (tens to hundreds of seconds), we may be able to reduce the requirements for the retroreflector target, and provide a capability for even more robust systems.

The future system will utilize a newly developed supercontinuum source capable of extending the operational wavelength range into the midwave infrared. The ground level differential absorption measurements with a midwave supercontinuum source transmitter will greatly expand supercontinuum absorption spectroscopy. Improved discrimination of target species, reduced false positive identification, and measurements at lower concentrations are expected with operations of a system operating in the midwave infrared; primarily due to the rich absorption spectra of many interesting species present there. The measurements are expected to expand the capability of detection techniques available for hydrocarbon compounds, which are of interest to the Departments of Energy (DOE) and Transportation (DOT) because of concerns regarding pipeline leaks. The Departments of Defense (DOD) and Homeland Security (DHS) are seeking solutions, such as this technique would offer, for detection of toxic chemicals, explosives, and chem-bio agents. Additionally, since the human eye is blind to midwave radiation, and the Earth-Sun radiance is minimal in this region, the system will be ideally suited for many environmental applications that monitor air quality in cities and in industrial complexes.

Acknowledgments

The authors would like to thank Joe Begnoché (PSU-MS) for his initial work with the laboratory measurements, and Qian Xu for her assistance with the atmospheric path SAS measurements. Additionally, the authors acknowledge the great importance of the work of

Gail Anderson, Jim Chetwynd and Michael Hoke and the host of contributors, past and present, who developed the MODTRANTM models.